I&EC research
Industrial & Engineering Chemistry Research

Separations

Hydrogen Separation at High Temperature with Dense and Asymmetric Membranes based on PIM-EA(H2)-TB/PBI Blends

Javier Sanchez-Lainez, Beatriz Zornoza, Mariolino Carta, Richard Malpass-Evans, Neil B. McKeown, Carlos Téllez, and Joaquin Coronas

Ind. Eng. Chem. Res., **Just Accepted Manuscript** • DOI: 10.1021/acs.iecr.8b04209 • Publication Date (Web): 12 Nov 2018

Just Accepted

ACS Publications

is published by the American Chemical Society. 1155 Sixteenth Street N.W., Washington, DC 20036

Hydrogen Separation at High Temperature with Dense and Asymmetric Membranes based on PIM-EA(H_2)-TB/PBI Blends

Javier Sánchez-Laínez[1], Beatriz Zornoza[1], Mariolino Carta[2], Richard Malpass-Evans[2], Neil B. McKeown[2], Carlos Téllez[1] and Joaquín Coronas[1*]

[1]Chemical and Environmental Engineering Department, Instituto de Nanociencia de Aragón (INA), Universidad de Zaragoza, 50018 Zaragoza, Spain.

[2]EastChem, School of Chemistry. University of Edinburgh. David Brewster Road, Edinburgh, EH9 3FJ (UK).

ABSTRACT: The preparation of dense and asymmetric flat membranes from the blending of polybenzimidazole (PBI) and (1.5-20 wt%) of a polymer of intrinsic microporosity (PIM-EA(H_2)-TB) is reported. Thermal characterization validated the blend by revealing a single glass transition temperature, which suggests the absence of polymer phase segregation. In addition, the decomposition activation energy and *d*-spacing of the blends follow trends that correlate with the amount of the PIM component. The membranes have been tested for the separation of H_2/CO_2 mixtures. The properties of the dense membranes, which also incorporate zeolitic imidazolate-8 (ZIF-8) nanoparticles, helped understanding of the behavior of the PIM/PBI blends by which phase inversion results in high separation performance asymmetric membranes. Asymmetric membranes show H_2/CO_2 selectivities of 23.8 (10/90 wt% PIM/PBI) and 19.4 (20/80 wt% PIM/PBI) together with respective H_2 permeances of 57.9 and 83.5 GPU at 250 °C and 6 bar feed pressure. The gas separation performance of these asymmetric blends has been fitted to an empirical model, showing the influence of the amount of PIM and the feed pressure.

INTRODUCTION

Membranes are an energy efficient technology for gas separation and purification compared to other technologies, such as those based on distillation and absorption processes. Due to their low energy cost and separation efficiency, as well as their small footprint and reliability, membranes units operate at

large- and small-scale, across the globe, for liquid and gas phase separations. However, polymeric membranes show limitations in their gas separation performance, especially due to their relatively low permeance and limited operating temperature.[1] Several solutions have been proposed to develop high-performance gas separation membranes, among which polymer blending and the preparation of mixed matrix membranes (MMMs) are of particular importance. The blending of polymers seeks the synergistic combination of different materials that can overcome their individual deficiencies. Miscible polymer blends are desirable to prepare homogeneous membranes with uniform and stable thermal and mechanical properties.[2] MMMs consist of embedded particles (i.e. fillers, which are often crystalline and porous) within a processable polymer matrix within a polymeric phase. Various polymers have been modified with inorganic fillers, such as zeolites or mesoporous silicas,[3,4] and metal organic frameworks (MOFs) [5-7] to enhance their gas separation performance.

The H_2/CO_2 separation has special relevance to hydrogen production and pre-combustion carbon capture. Many advances have been recently published on materials and membranes for this separation at high temperature.[8-11] Polybenzimidazole (PBI) is a polymer widely used to prepare membranes for H_2/CO_2 separation.[12-17] It possesses high thermal and chemical stabilities, good mechanical resistance and a high intrinsic H_2/CO_2 selectivity. Nevertheless, its main disadvantages are low permeability and brittleness.[18] On the contrary, polymers of intrinsic microporosity (PIMs) display huge H_2 permeability as self-standing films often well in excess of 1000 Barrer (1 Barrer = 10^{-10} cm^3(STP) cm cm^{-2} s^{-1} $cmHg^{-1}$) but with limited size selectivity for H_2 over CO_2 due to the relatively large voids present in their structure.[19] The fabrication of a film from the blend of both PBI and a PIM might result in one membrane with good H_2/CO_2 selectivity and enhanced permeability. PBI has already been blended with polyimides, such as Matrimid®,[20,21] P84®,[22] DPPD-IMM[23] or Torlon®,[20,22] obtaining interesting gas separation performance. The good miscibility between PBI and the polyimides is obtained thanks to the affinity between the N-H of the former and the C=O of the latter, allowing the formation of hydrogen bonds.[24] The polyimide segments reinforced the mechanical strength of the membranes while the PBI chains increased their thermal stability. Blends of PBI can also be found in the literature with polyaniline,[25] and polyvinylidene fluoride (PVDF).[26] PIMs have also been blended with polyimides.[27-31] For instance, PIM-1 has been mixed with Matrimid® with even low amounts (~ 10 wt%) increasing permeability by ~75 % with a minimal reduction of CO_2/CH_4 selectivity.[32] PIM-1 has also been blended with polyethylene glycol (PEG) giving excellent results for the separation of CO_2/N_2 and CO_2/CH_4 mixtures, superior to those of neat PIM-1,

with CO_2 permeabilities close to 2000 Barrer and CO_2/N_2 and CO_2/CH_4 selectivities of 16 and 39, respectively.[33] The blending of PIM-1 with sulfonated polyphenylenesulfone (sPPSU) can also be found in the literature.[34,35] The increase in the degree of sulfonation in sPPSU/PIM-1 blends led to a decrease in chain–chain packing, and therefore an enhancement in the CO_2/CH_4 selectivity.[35]

In this work we show the preparation of dense and asymmetric flat membranes from the blending of PBI and PIM-EA(H_2)-TB at different proportions. PIM-EA(H_2)-TB contains ethanoanthracene (EA) components linked by Tröger-base (TB) (*2,8-dimethyl-6H,12H-5,11-methanol dibenzo[b,f][1,5]diazocina*).[36] It possesses an extremely rigid backbone that allows it to display a small selectivity for H_2 over CO_2 room temperature. Therefore, PIM-EA(H_2)-TB is more appropriate than other PIMs for blending to obtain membranes for H_2/CO_2 separation. Most of the blends involving PBI (and PIM-1) were implemented as dense membranes with the exception of Matrimid®-PBI[20,21] and PVDF-PBI,[26] what reinforces the novelty of this work. Moreover, ZIF-8 has been used as a porous filler to prepare MMMs with this blended polymer mixture as matrix. ZIF-8 is a zeolitic imidazolate framework with **sod** topology based on the coordination of Zn with the organic linker 2-methylimidazolate. It possesses cavities of 1.16 nm connected through pore windows of 0.34 nm.[36] This way, the permeance of H_2 is expected to be favored over that of CO_2 (kinetic diameter of 0.29 nm *vs.* 0.33 nm, respectively). The effects of composition, miscibility, microstructure and gas separation performance are investigated.

EXPERIMENTAL METHODS

Dense MMM film preparation

The required amount of PIM (synthesized as previously reported from the reaction of 2,6(7)-diaminoanthracene with dimethoxymethane in trifluoroacetic acid.[37-39])was weighed for each blending proportion, from 1.5 to 20 wt%, and dispersed in DMAc (Sigma Aldrich), stirring at room temperature until complete dissolution was obtained. PBI commercial solution (26 wt% concentration in DMAc, Celazole® S26) was added so that the final concentration of the polymer blend (*ca.* 40 mg in dry basis) in solvent was 10 wt% and the stirring was maintained overnight. The casting solution was sonicated three times for 15 min periods and then cast into a Petri dish, which was left uncovered and placed on a leveled surface inside an oven at 90 °C. Once dried, the films were peeled off from the Petri dishes and washed for 24 h in MeOH (HPLC grade, Scharlau). Finally, the membranes were activated in an oven at 100 °C for 24 h to remove any remaining traces of solvent. For the blends that incorporated ZIF-8

(prepared as nanoparticles in a MeOH/H_2O mixture[40]), the filler was dispersed in DMAc previous to the first addition of the PIM polymer. Pure PBI membranes were prepared following the same procedure without incorporating any PIM (see Table S1 for further details).

Pure PIM-EA(H_2)-TB membranes were prepared dissolving 40 mg of polymer in 3.6 g of chloroform (anhydrous, Sigma Aldrich). The casting solution was stirred overnight, then three times sonicated for 90 min in total and cast into a leveled Petri dish. The Petri dishes were left covered to allow a slow evaporation of the solvent at room temperature. After that, the membranes followed the same soaking and drying procedure as for the blends. Note that different solvents have been used depending on the membrane polymer. Even if PIM membranes could be affected by the casting solvent,[41] the typical solvents in which the membranes were prepared and optimized were preferred: DMAc for pure PBI and chloroform for PIM containing membranes. Besides, the alternatives to DMAc are similar harm solvents such as DMF or NMP, while PIMs can benefit from less toxic solvents.

The thickness of the membrane samples (88±16 μm) was measured with a Digimatic Micrometer Mitutoyo (measurement range from 0 to 30 mm with an accuracy of ±1 μm), considering the average of 9 values obtained at different places.

PBI asymmetric membranes preparation

PBI asymmetric membranes were prepared *via* phase inversion method. The corresponding amount of PIM was dissolved in DMAc according to the blending proportion, stirring at room temperature and the 26 wt% PBI commercial solution was added equally in three stages until the total amount was reached (see Table S1). The final concentration of the resulting polymer dope was 20 wt%. The casting solution was left still overnight to remove any bubbles present in it and cast on a P84® support[42] using the Elcometer 4340 Automatic Film Applicator and immediately immersed into a DI water bath at 25 °C. Afterwards, the membranes were rinsed in DI water for 72 h to remove all the DMAc and then with MeOH and *n*-hexane (Scharlau) for 90 min. Then the membranes were dried and healed immersing them in a coating solution of PDMS (Sylgard® 184). A 3 wt% coating solution in *n*-hexane was used mixing PDMS polymer base and hardener (10 to 1 weight ratio). The membranes were allowed to evaporate at room temperature for 2 h and then cured in an oven at 100 °C for 18 h. Neat PBI membranes were prepared following the same procedure and obtaining a 20 wt% dope solution from the dilution of the 26 wt% PBI commercial solution in DMAc.

Characterization of samples

Thermogravimetric analysis (TGA) was performed with a Mettler Toledo TGA/STDA 851e. Samples of 5 mg were placed in 70 µL aluminum pans that were heated in air atmosphere from 30 to 900 °C at heating rates of 5, 10 and 20 °C min^{-1}. Differential scanning calorimetry (DSC) analysis was carried out with a Mettler Toledo DSC822e. The 10 mg samples were placed in 70 µL aluminum pans and heated under 40 mL min^{-1} nitrogen flow from 25 to 500 °C using a heating rate of 20 °C min^{-1}. Scanning electron microscopy (SEM) images were acquired with an Inspect F50 model scanning electron microscope (FEI), operated at 20 kV and using a coating of Pt. The cross-sections of the membranes were prepared fracturing the samples during their immersion in liquid nitrogen. Infrared analysis (FTIR) was performed on a Bruker Vertex 70 FTIR spectrometer, which used a Golden Gate diamond ATR accessory and a DTGS detector, and with the FTIR microscope HYPERION 2000. The spectra were recorded by averaging 40 scans in the 4000-600 cm^{-1} wavenumber range at a resolution of 4 cm^{-1}. Powder X-ray diffraction (XRD) spectra of ZIF-8 and MMMs were obtained with a D-Max Rigaku X-ray diffractometer that used a copper anode and a graphite monochromator to select CuKα radiation (λ = 1.540 Å). Data from 2θ=2.5° to 40° were taken at a scan rate of 0.03° s^{-1}.

Gas separation analysis

The membranes, consisting in circular areas of 2 cm diameter, and sealed with silicon o-rings, were placed in a permeation module based on two stainless steel pieces and a 316LSS macroporous disk support (from Mott Co.) with a 20 µm nominal pore size. This module was placed in an UNE 200 Memmert oven that controlled the temperature of the experiment. The gas separation tests were performed feeding a 25/25 cm^3(STP) min^{-1} H_2/CO_2 mixture maintaining 3-6 bar at the feed side using two mass-flow controllers (Alicat Scientific, MC-100CCM-D), one for each gas. At the same time, Ar at 1 bar was used as sweep gas at the permeate side of the membrane, with a flow of 2-10 cm^3(STP) min^{-1} controlled by a mass-flow controller (Alicat Scientific, MC-5CCM-D and MC-100CCM-D). The concentration of H_2 and CO_2 in the permate were analyzed online with an Agilent 3000A gas microchromatograph using a thermal conductivity detector (TCD). After at least 3 h and once the steady-state was reached, the permeability was calculated in Barrer (10^{-10} cm^3(STP) cm cm^{-2} s^{-1} $cmHg^{-1}$) and the separation selectivity as the ratio of permeabilities. For asymmetric membranes permeance was calculated instead in GPU (10^{-6} cm^3(STP) cm^{-2} s^{-1} $cmHg^{-1}$). At least 2-3 membranes of each type were measured to provide the corresponding standard deviations.

RESULTS AND DISCUSSION

Membrane characterization

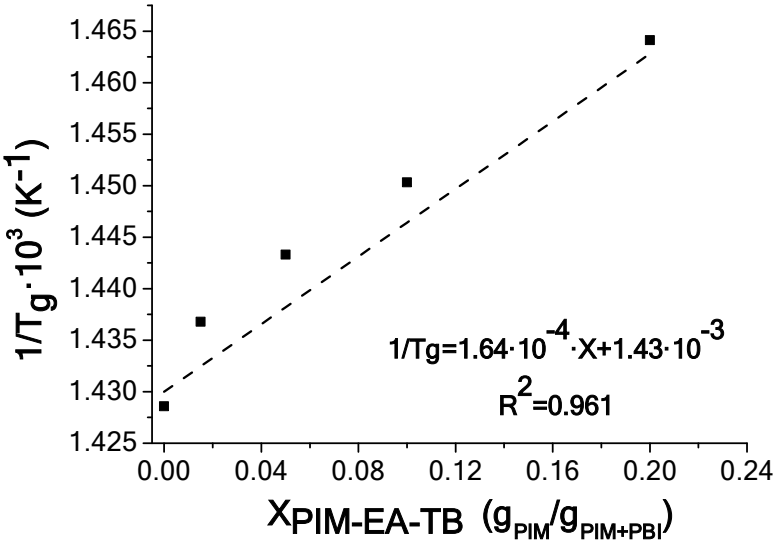

Figure 1. Glass transition temperature (T_g) values of the blends (scatters) as a function of the amount of PIM-EA(H_2)-TB in them and its fitting to the Fox equation (dashed line).

The polymers PBI and PIM-EA(H_2)-TB have been combined where the latter is the minor component in the blend. Two polymers are considered to have built a homogenous blending when they possess a single gas transition temperature (T_g), indicating the full miscibility of the system at the molecular level.[43] Blends of PBI and PIM-EA(H_2)-TB were prepared using amounts of PIM from 1.5 to 10 wt% and the T_g of the different membranes was calculated from DSC data (see Table S2). The increase of the amount of PIM in the blend implies a reduction in the T_g of the membrane, almost following an arithmetic sequence.

The theoretical T_g of a polymer blend can be calculated with the Fox equation (Equation 1).[44]

$$\frac{1}{T_{g,blending}} = \frac{X_{PIM-EA(H_2)-TB}}{T_{g,\,PIM-EA(H_2)-TB}} + \frac{(1-X_{PIM-EA(H_2)-TB})}{T_{g,PBI}} \quad (1)$$

where $T_{g,PIM\text{-}EA(H_2)\text{-}TB}$ and $T_{g,PBI}$ are the glass transition temperatures in K of the individual polymers and $X_{,PIM\text{-}EA(H_2)\text{-}TB}$ and $X_{,PBI}$ are related to the mass fractions of each component in the blend. For this case of study, this equation cannot be directly applied because the T_g of PIM-EA(H_2)-TB is unable to be measured empirically, its value being higher than the degradation temperature of the polymer. Reorganizing the equation, it can be expressed as Equation 2. This way, the T_g of the blends should follow a linear tendency when represented against the amount of PIM in the composite.

$$\frac{1}{T_{g,blending}} = \left(\frac{1}{T_{g,\,PIM-EA(H_2)-TB}} - \frac{1}{T_{g,\,PBI}}\right)\cdot X_{PIM-EA(H_2)-TB} + \frac{1}{T_{g,PBI}} \quad (2)$$

As seen in Figure 1, the measured values fit to this reorganized Fox equation and, according to this fitting, the calculated T_g value for neat PBI is 426 °C, meaning 0.2% error in comparison with its empirical value (427 °C, see Table S2). Besides, a hypothetical T_g for PIM-EA(H_2)-TB of 354 °C can also be obtained.

Thermogravimetric analyses in air were performed using three different heating rates of 5, 10 and 20 °C min^{-1} with bare PBI membranes and blends containing a 5 and 10 wt% of PIM-EA(H_2)-TB. The temperatures corresponding to the maximum weight loss were obtained from the derivative curve of each thermogram (Figure S1) and they are collected in Table S3. It can be seen that the presence of PIM accelerated the thermal decomposition of the blend. The apparent activation energy (E_a) of these reactions was calculated for the different membranes using the Kissinger integral method.[45] The temperatures shown in Table S3 were represented and fitted according to the Kissinger equation (Equation S3) in Figure S2. The incorporation of PIM in the blend is responsible for a significant reduction in the E_a (105, 87 and 83 kJ mol^{-1} for 0, 5 and 10 wt% PIM in the blend, respectively), since just a 5 wt% of polymer makes this parameter decrease by a 17%. This agrees with a decrease of the polymer thermal stability as PBI is replaced by the PIM. In general, the lower the T_g value of a given polymer the higher its E_a value should be: e.g. *ca.* 190 °C (T_g) and 285 kJ mol^{-1} (E_a) for typical polysulfone.[46] Noteworthy, the TGA results may not show the true thermal stability of the membranes because the presence of oxygen could accelerate the decomposition or oxidation of certain functionalities. Besides, from the TGA analysis (see Figure S1) it can also be notice that all the DMAc drove out by water during the membrane activation process.

FTIR spectroscopy can show the interaction of polymers in a blended structure. New vibration modes are usually detected when blends mean new strong interactions in terms of covalent bonds. A physical blending without any chemical reaction, i.e. involving only van der Waals, electrostatic or hydrogen interactions, would not produce new FTIR vibrations. Figure S3 spectra show the signals at 757 cm^{-1} and those at 1221-1120 cm^{-1}, present in the neat PBI spectrum and corresponding to in-plane bending of the imidazole and benzene rings, respectively.[47] These bands decreased in intensity in the blends. However, no new signals different from those of the bare polymer membranes could be found. This means that the interaction between PBI and the PIM follows the same kind of bonding already found in the neat polymers, which is logical since they have similar functional groups. FTIR analysis was also performed

with a FTIR microscope, measuring several areas of 30 μm x 30 μm on the membrane surface of the blend with 20 wt% of PIM (see Figure S4). The homogeneity among the different spectra confirmed the intimate mixing between PIM-EA(H2)-TB and PBI, without segregation at a micron scale.

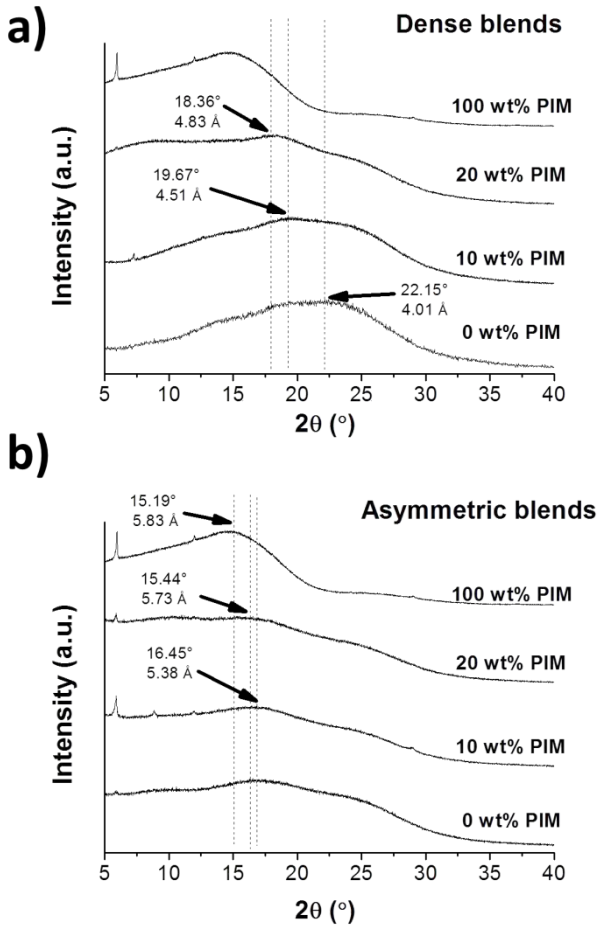

Figure 2. XRD patters of membranes: bare PBI, bare PIM-EA(H_2)-TB and blends containing 10 and 20 wt% of PIM, in dense (a) and asymmetric configurations (b).

An XRD analysis was performed to gain insight into the effect of the blending on the microstructure and to obtain the *d*-spacing of the membranes. As shown in Figure 2, PBI is an amorphous polymer with an indicative band at $2\theta = 22.2°$, corresponding to a *d*-spacing of 4.0 Å. PIM-EA(H_2)-TB is a glass polymer, an amorphous band at 15.2°. As shown in Figure 2a, in the case of dense membranes an increase in the PIM concentration gradually shifted the peak at 22.2^0 to lower values, increasing the interstitial space between the polymer chains up to 4.8 Å. In the case of asymmetric membranes (Figure 2b) the signal at 16.5° of PIM-EA(H_2)-TB was more visible and it shifted to higher values with the decrease in the amount of PIM in the blend, showing again that the space between the polymer chains in the blend is higher with increasing PIM loading. The spectrum of PIM-EA(H_2)-TB in both figures corresponds to that of the

dense membrane. It was impossible to prepare a pure PIM-EA(H_2)-TB asymmetric membrane due to the difficulty to dissolve this polymer in DMAc at high loadings, which is necessary for the preparation of a defect-free asymmetric film. No XRD signals related to PIM-EA(H_2)-TB could be noticed in the patterns of the blends with 1.5 and 5 wt% of PIM (in line with the fact that the 10 wt% sample already showed low XRD intensities) and they were not included in Figure 2.

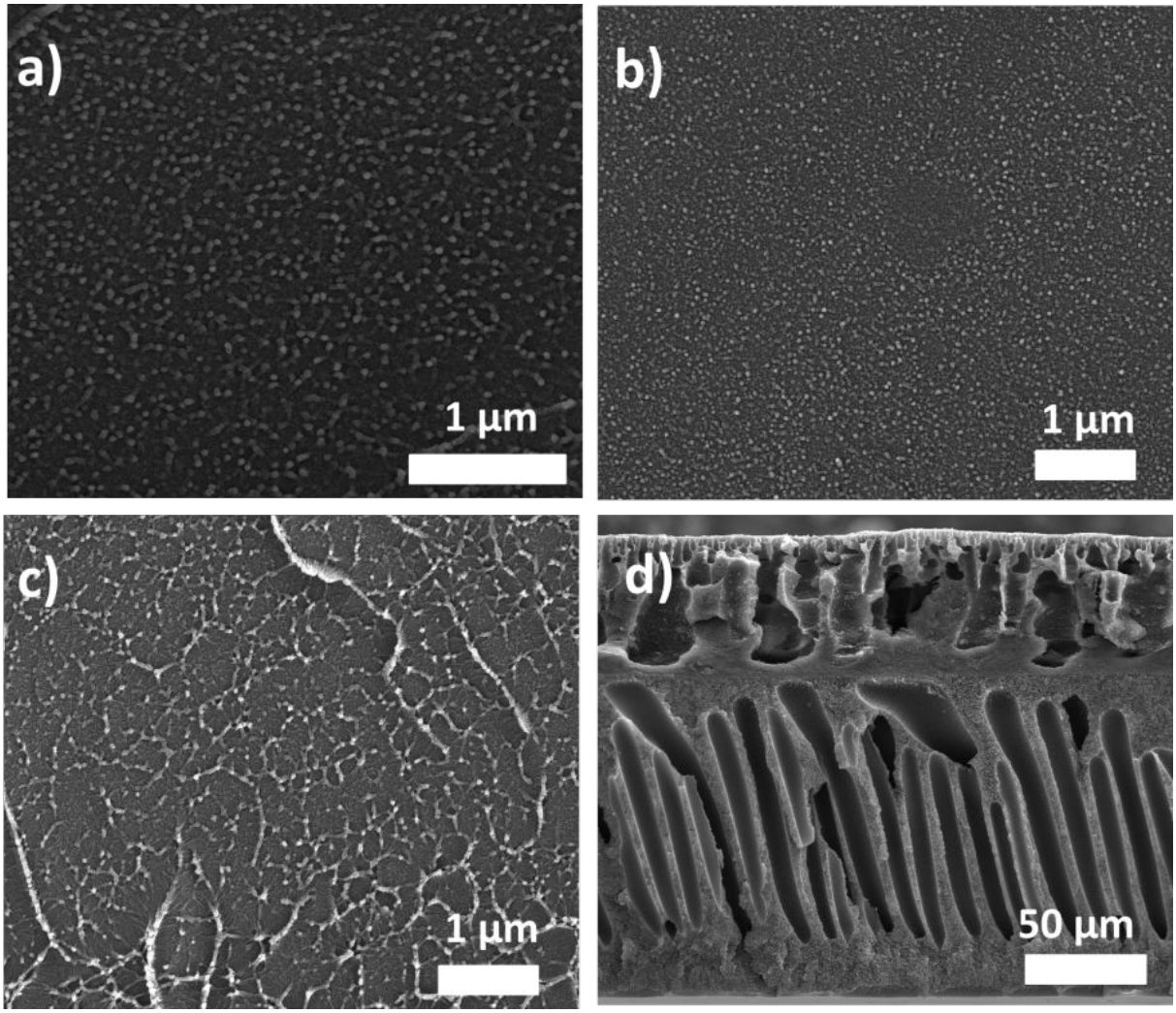

Figure 3. SEM images of the cross section of membranes: bare PBI (a), neat PIM-EA(H_2)-TB (b) and blend with 10 wt% of PIM in dense (c) and asymmetric configuration (d).

Finally, Figure 3 shows the cross-sections of membranes of bare PBI, neat PIM-EA(H_2)-TB and the blend containing 10 wt% of PIM in both dense and asymmetric morphology. The appearance and texture of both neat polymers is quite similar, being difficult to distinguish one another. Besides, the image of the blend looks homogeneous, with no phase separation. The images of the blends containing ZIF-8 are

shown in Figure S5, where the filler can be seen homogenously dispersed across the section for all loadings.

Gas separation performance of dense membranes

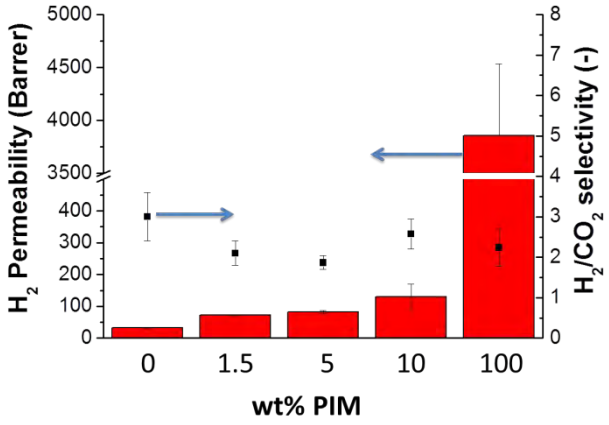

Figure 4. Gas separation performance of dense membranes at 180 ^{0}C and 3 bar of pressure feed: pristine polymers and blends with different PIM-EA(H_2)-TB loadings. Bars stand for H_2 permeability and scatter for H_2/CO_2 selectivity.

The gas separation performance of dense membranes, blends in absence of filler, at 180°C and 3 bar of feed pressure can be seen in Figure 4. The numerical values are also collected in Table S4 PIM-EA(H_2)-TB (100 wt% PIM) shows a tremendous high H_2 permeability, 100 times that of PBI with 3857 Barrer, but poor H_2/CO_2 selectivity (*ca.* 2.2).

Blends at 1.5, 5 and 10 wt% of PIM increased the H_2 permeability of the PBI from 31.9 to 72.2, 82.0 and 131 Barrer, respectively, but did not improve the membrane selectivity, since that of neat PIM-EA(H_2)-TB was not very high (2.2). This may be related to the increase in the *d-spacing* previously observed by XRD (see Figure 2). ZIF-8 nanoparticles were also added to the blended matrix in an attempt to enhance the separation performance of the membranes (see Table S4) All the results of dense membranes are represented in a Robeson type graph (Figure S6) where it can be seen that the best performing membranes surpass the Robeson upper bound corrected for 180 °C. Table S5 also shows the gas separation performance of dense membranes found in the literature for comparison; in general, the selectivity values with dense membrane are below those achieved with asymmetric membranes for this particular separation.

Gas separation performance of asymmetric membranes

In order to study in depth, the effect of PIM-EA(H_2)-TB/PBI blends in the gas separation performance of H_2/CO_2 mixtures, a new membrane configuration based on asymmetric blended membranes was tested. ZIF-8 was not incorporated in this kind of membranes because it did not achieved sufficient improvement with the previous dense blends. The higher permeances of this kind of membranes in comparison with those of dense blends allowed the measurements at several temperatures from 35 to 250 °C. Different feed pressures up to 6 bar were also applied (see Table S6). The membranes were prepared on P84® flat asymmetric supports and the results were compared with those corresponding to pristine PBI membranes of this kind previously reported.[42] The use of P84® is necessary because PBI asymmetric blends are extremely brittle and impossible to handle without the use of a support. This polymer has been selected for this purpose because of its compatibility with PBI, which allows the absence of delamination in the composite.[48] In order to discard a possible contribution of P84® to the gas separation, a PBI supported blend (10 wt% PIM) has also been tested for a different gas separation (i.e. equimolar CO_2/CH_4 mixture) at 35 °C and a feed pressure of 3 bar, showing a CO_2 permeance of 0.42 GPU and a CO_2/CH_4 selectivity of 1.4. Such a low selectivity proves that only the PBI layer is playing a role in the gas separation, because P84® usually shows a high CO_2/CH_4 selectivity while that of PBI is negligible.[49]

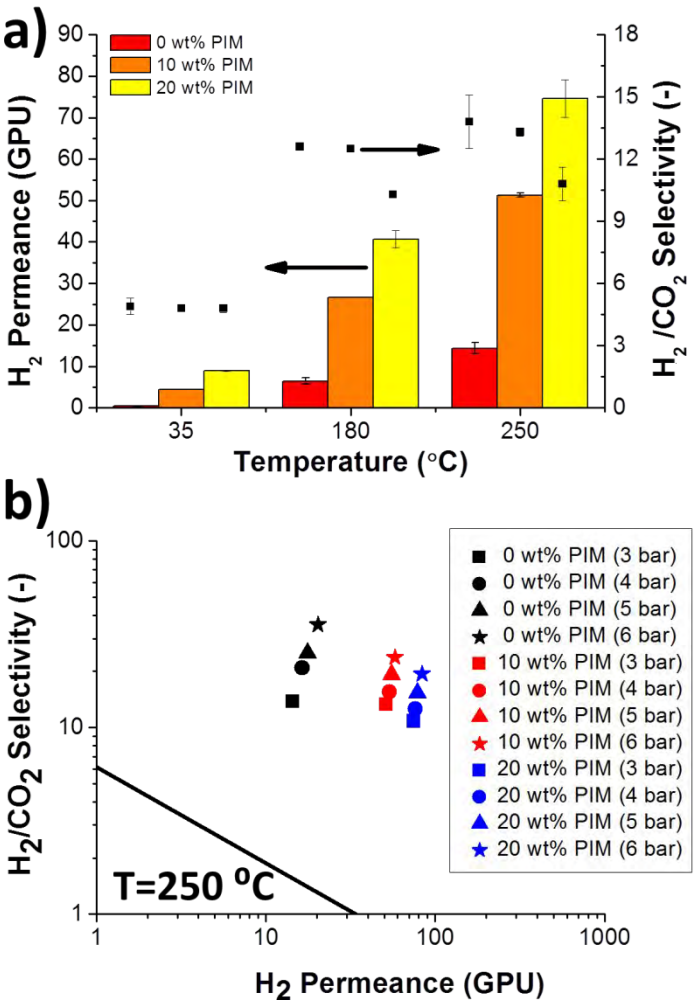

Figure 5. Gas separation performance of asymmetric blends: (a) at several operating temperatures and 3 bar of feed pressure (bars stands for H_2 permeance and scatter for H_2/CO_2 selectivity); and (b) gas separation performance at 250 ^{0}C and different feed pressures with the H_2/CO_2 upper bound at the same temperature.

Figure 5a shows the gas separation performance of asymmetric PBI membranes (pristine polymer and blends containing 10 and 20 wt% of PIM. Asymmetric membranes with 1.5 and 5 wt% of PIM were not prepared because such low loading did not show a considerable improvement with the previous dense membranes (see Figure 4). The entire test was performed under a feed pressure of 3 bar and temperatures of 35, 180 and 250 °C. When these results are compared to those in Figure 4, the asymmetric membranes show a better gas separation performance than the dense membranes, presumably due to the different polymeric structure of the skin layer (less porous).[42] The content of PIM in the blends provided an enhancement in the H_2 transport. At 35 °C the H_2 permeance increased from 0.4 to 8.9 GPU (22 times higher) when the content of PIM increased from 0 to 20 wt%. At higher temperatures the increase in permeance was even greater, reaching the maximum H_2 permeance of 74.6 GPU for the blend containing

20 wt% of PIM at 250 °C. Conversely, the H_2/CO_2 selectivity decreased slightly as the amount of PIM in the blend was increased, as previously seen for dense membranes, but H_2/CO_2 selectivity remained over 10 at the highest temperature. Increasing the operating temperature had a great impact on the H_2 permeation in all bare PBI membranes and blends. The H_2 permeance was around 5 times higher at 180 °C than at 35 °C (from 0.4-8.9 GPU to 6.5-40.7 GPU) and twice at 250 °C than at 180 °C (from 6.5-40.7 GPU to 14.4-74.6 GPU). The H_2/CO_2 selectivity also improved as the temperature rose, being 2.5-fold higher at 180 °C in comparison with that at the lowest temperature (4.8), and it even increased further when measuring at 250 °C (13.8). Measuring at different temperatures also allowed the calculation of the apparent activation energies of the membranes in terms of permeances for H_2 and CO_2 (see Figure S5 and Table S7). Calculated from H_2 permeances, pristine PBI membranes showed an apparent activation energy of 22.3 kJ mol^{-1}, a value that decreased to 14.9 and 13.9 kJ mol^{-1} as the amount of PIM increased to 10 and 20 wt%, respectively. The same happened with the values calculated from CO_2 permeances, which decreased from 15.6 to 7.6 kJ mol^{-1}. This activation energy shows the same tendency as that (corresponding to membrane stability) calculated by thermal analysis, previously shown in Figure S2. Since thermal treatments have been reported to be able to affect the transport properties of PIMs,[36] the blend with 20 wt% of PIM was measured again after cooling down the membrane to room temperature. Its gas separation performance (see Table S6) was similar to the original at 250 °C, showing that the high temperature operation had almost no effect on the gas separation properties of the blend.

Regarding the effect of pressure on the gas separation performance of the membranes, Figure 5b shows the separation selectivity results of PBI blends at 250 °C under feed pressures from 3 to 6 bar. As previously reported,[42] the increase in the feed pressure led to an enhancement of the gas separation performance. The disappearance of defects thanks to the membrane healing by PDMS coating together with the small thickness of their skin layer probably caused the membranes to reach CO_2 saturation, significantly increasing the gas transport and the separation factor, as observed in case of pure PBI membranes.[42] The effect of pressure was less significant as the amount of PIM in the blend increased. For bare PBI membranes, the H_2 permeance was 29 % higher at 6 bar than at 3 bar and the H_2/CO_2 selectivity 61 % higher, reaching values of 20.3 GPU and 35.6, respectively. However, for both blends, the H_2 permeance increased by 10 % and the selectivity by 44 %. The best values for the blends were obtained at 6 bar feed pressure with 57.9 GPU of H_2 and a H_2/CO_2 selectivity of 23.8 (10 wt% of PIM) and 83.5 GPU

of H_2 and a H_2/CO_2 selectivity of 19.4 (20 wt% of PIM). All the permselectivity results surpass clearly the H_2/CO_2 upper bound defined in GPU at 250 °C.[42]

It can also be shown that the gas separation performance of the asymmetric blends follows a linear tendency based on the amount of PIM in the composite and the feed pressure of the process. The values of H_2 and CO_2 permeances shown in Figure 5b were fitted by multiple linear regression, providing the empirical model described by Equations 3 and 4. No physical meaning is under these expressions as far as we are concerned. The fitting was successful (R^2 value > 0.97) and can be seen in Figure S5.

$$\boldsymbol{P_{H_2} = 9.11 + 3.05 \cdot loading\ (wt\%) + 2.30 \cdot P\ (bar)} \quad \textbf{(3)}$$

$$\boldsymbol{P_{CO_2} = 3.03 + 0.24 \cdot loading\ (wt\%) - 0.50 * P\ (bar)} \quad \textbf{(4)}$$

From the model, it can be seen how increasing the PIM content (*loading*) in the blend provides increases in gas transport for both H2 and CO2, since it is a positive term in both previous equations. The feed total pressure (*P*), however, has a different influence for each gas. Increasing this variable leads to simultaneous increase and decrease of the H_2 and CO_2 permances, respectively. This fact is due to the saturation phenomena already explained above and supports the enhancement of the H_2/CO_2 with increasing pressure.

CONCLUSIONS

Blends of PBI and PIM-EA(H_2)-TB have been prepared in both dense and asymmetric configurations. The formation of a homogeneous blend between the two polymers was verified by the existence of a single glass transition temperature. The incorporation of PIM into PBI made the *d*-spacing of the resulting polymer increase, leading to higher gas permeances. The apparent activation energies of the blends, for thermal degradation and permeation, decreased as the amount of PIM in the composite was higher. The PIM/PBI blends were tested for the separation of H_2/CO_2 mixtures. Dense membranes also incorporated ZIF-8 nanoparticles to try to improve the gas separation thanks to the molecular sieving effect of this filler. The combination of PIM and PBI enhanced greatly the permeability of the membranes but reduced selectivity, due to the poor H_2/CO_2 separation selectivity of PIM-EA(H_2)-TB. Asymmetric blends performed much better than the dense membranes due to their thin skin layer. With these composites, the increase in feed pressure had a positive effect on the gas separation performance, reaching a maximum H_2 permeance of 83.5 GPU with a H_2/CO_2 selectivity of 19.4. The empirical model developed corroborated the influence of the amount of PIM and the feed pressure on the gas separation

performance. Finally, the presence of characterization and separation results with both dense and asymmetric membranes of the PIM-1/PBI blend allows an interesting comparison not usually afforded in membrane gas separation publications. This allows to envisage the great potential that blends of high performance polymers may have in the separation of H_2/CO_2 mixtures.

Supporting Information.

Information about the thermal analysis, the characterization of membrane samples and gas separation is included. This material is available free of charge via the Internet at http://pubs.acs.org.

ACKNOWLEDGEMENTS

The research comprising this work has received financial support from the European Union Seventh Framework Programme (FP7/2007-2013) under grant agreement n° 608490, project M4CO2. Besides, the authors thank the funding received from the Spanish MINECO and FEDER (MAT2016-77290-R), the Aragón Government (T43-17R) and the European Social Fund. J. S-L. in particular thanks the Spanish Education Ministry Program FPU2014. All the microscopy work was performed in the Laboratorio de Microscopías Avanzadas at the Instituto de Nanociencia de Aragón (LMA-INA). Finally, the authors would like to acknowledge the use of the Servicio General de Apoyo a la Investigación-SAI, Universidad de Zaragoza.

AUTHOR INFORMATION

Corresponding Author

*Email: coronas@unizar.es (J.C.).

Notes

The authors have no competing financial interest to declare.

REFERENCES

(1) Robeson, L. M. The upper bound revisited. *J. Membr. Sci.* **2008**, *1*, 390-400.

(2) Chung, T.; Guo, W. F.; Liu, Y. Enhanced Matrimid membranes for pervaporation by homogenous blends with polybenzimidazole (PBI). *J. Membr. Sci.* **2006**, *1*, 221-231.

(3) Zornoza, B.; Irusta, S.; Téllez, C.; Coronas, J. Mesoporous silica sphere− polysulfone mixed matrix membranes for gas separation. *Langmuir* **2009**, *10*, 5903-5909.

(4) Mahajan, R.; Burns, R.; Schaeffer, M.; Koros, W. J. Challenges in forming successful mixed matrix membranes with rigid polymeric materials. *J. Appl. Polym. Sci.* **2002**, *4*, 881-890.

(5) Jeazet, H. B. T.; Staudt, C.; Janiak, C. Metal–organic frameworks in mixed-matrix membranes for gas separation. *Dalton Trans.* **2012**, *46*, 14003-14027.

(6) Rodenas, T.; van Dalen, M.; García-Pérez, E.; Serra-Crespo, P.; Zornoza, B.; Kapteijn, F.; Gascon, J. Visualizing MOF Mixed Matrix Membranes at the Nanoscale: Towards Structure-Performance Relationships in CO_2/CH_4 Separation Over NH2-MIL-53 (Al)@ PI. *Adv. Funct. Mater.* **2014**, *2,* 249-256.

(7) Sabetghadam, A.; Seoane, B.; Keskin, D.; Duim, N.; Rodenas, T.; Shahid, S.; Sorribas, S.; Guillouzer, C. L.; Clet, G.; Tellez, C. Metal Organic Framework Crystals in Mixed-Matrix Membranes: Impact of the Filler Morphology on the Gas Separation Performance. *Adv. Funct. Mater.* **2016,** *26,* 3154–3163.

(8) Smart, S.; Vente, J. F.; Diniz da Costa, J. C. High temperature H2/CO2 separation using cobalt oxide silica membranes, *Int. J. Hydrogen Energy* **2012**, *17,* 12700-12707.

(9) Japip, S.; Liao, K.; Chung, T. Molecularly tuned free volume of vapor cross-linked 6FDA-Durene/ZIF-71 MMMs for H_2/CO_2 separation at 150° C. *Adv. Mater.* **2017**, *4,* 1603833.

(10) Jang, E.; Kim, E.; Kim, H.; Lee, T.; Yeom, H.; Kim, Y.; Choi, J. Formation of ZIF-8 membranes inside porous supports for improving both their H_2/CO_2 separation performance and thermal/mechanical stability, *J. Membr. Sci.* **2017**,*540,* 430-439.

(11) Zhu, X.; Wang, Q.; Shi, Y.; Cai, N. Layered double oxide/activated carbon-based composite adsorbent for elevated temperature H_2/CO_2 separation, *Int. J. Hydrogen Energy* **2015**, *30,* 9244-9253.

(12) Choi, S.; Coronas, J.; Lai, Z.; Yust, D.; Onorato, F.; Tsapatsis, M. Fabrication and gas separation properties of polybenzimidazole (PBI)/nanoporous silicates hybrid membranes. *J. Membr. Sci.* **2008**, *1,* 145-152.

(13) Yang, T.; Xiao, Y.; Chung, T. Poly-/metal-benzimidazole nano-composite membranes for hydrogen purification. *Energy Environ. Sci.* **2011**, *10,* 4171-4180.

(14) Li, L.; Jianfeng, Y.; Wang, X.; Chen, Y.; Wang, H. ZIF-11/Polybenzimidazole composite membrane with improved hydrogen separation performance. *J. Appl. Polym. Sci.* **2014**, 41056.

(15) Li, X.; Singh, R. P.; Dudeck, K. W.; Berchtold, K. A.; Benicewicz, B. C. Influence of polybenzimidazole main chain structure on H_2/CO_2 separation at elevated temperatures. *J. Membr. Sci.* **2014**, *461,* 59-68.

(16) Kumbharkar, S.; Liu, Y.; Li, K. High performance polybenzimidazole based asymmetric hollow fibre membranes for H_2/CO_2 separation. *J. Membr. Sci.* **2011**, *1,* 231-240.

(17) Biswal, B. P.; Bhaskar, A.; Banerjee, R.; Kharul, U. K. Selective interfacial synthesis of metal–organic frameworks on a polybenzimidazole hollow fiber membrane for gas separation. *Nanoscale* **2015**, *16,* 7291-7298.

(18) Chung, T. A critical review of polybenzimidazoles: historical development and future R&D. *J. Macromol. Sci. Part C: Polym. Rev.* **1997**, *2,* 277-301.

(19) Budd, P. M.; McKeown, N. B. Highly permeable polymers for gas separation membranes. *Polym. Chem.* **2010**, *1,* 63-68.

(20) Hosseini, S. S.; Teoh, M. M.; Chung, T. S. Hydrogen separation and purification in membranes of miscible polymer blends with interpenetration networks. *Polymer* **2008**, *6,* 1594-1603.

(21) Hosseini, S. S.; Peng, N.; Chung, T. S. Gas separation membranes developed through integration of polymer blending and dual-layer hollow fiber spinning process for hydrogen and natural gas enrichments. *J. Membr. Sci.* **2010**, *1*, 156-166.

(22) Hosseini, S. S.; Chung, T. S. Carbon membranes from blends of PBI and polyimides for N_2/CH_4 and CO_2/CH_4 separation and hydrogen purification. *J. Membr. Sci.* **2009**, *1*, 174-185.

(23) Pérez-Francisco, J. M.; Santiago-García, J. L.; Loria-Bastarrachea, M. I.; Aguilar-Vega, M. Evaluation of Gas Transport Properties of Highly Rigid Aromatic PI DPPD-IMM/PBI Blends. *Ind. Eng. Chem. Res.* **2017**, *33*, 9355-9366.

(24) Musto, P.; Karasz, F.; MacKnight, W. Hydrogen bonding in polybenzimidazole/poly (ether imide) blends: a spectroscopic study. *Macromolecules* **1991**, *17*, 4762-4769.

(25) Giel, V.; Morávková, Z.; Peter, J.; Trchová, M. Thermally treated polyaniline/polybenzimidazole blend membranes: Structural changes and gas transport properties. *J. Membr. Sci.* **2017**, *537*, 315-322.

(26) Ahmad, N.; Leo, C.; Ahmad, A.; Mohammad, A. W. Separation of CO_2 from hydrogen using membrane gas absorption with PVDF/PBI membrane. *Int. J. Hydrogen Energy* **2016**, *8*, 4855-4861.

(27) Yong, W. F.; Li, F. Y.; Xiao, Y. C.; Chung, T. S.; Tong, Y. W. High performance PIM-1/Matrimid hollow fiber membranes for CO_2/CH_4, O_2/N_2 and CO_2/N_2 separation. *J. Membr. Sci.* **2013**, *443*, 156-169.

(28) Yong, W. F.; Salehian, P.; Zhang, L.; Chung, T. Effects of hydrolyzed PIM-1 in polyimide-based membranes on C2–C4 alcohols dehydration via pervaporation. *J. Membr. Sci.* **2017**, *523*, 430-438.

(29) García, M. G.; Marchese, J.; Ochoa, N. A. Improved gas selectivity of polyetherimide membrane by the incorporation of PIM polyimide phase. *J. Appl. Polym. Sci.* **2017**,44682.

(30) Salehian, P.; Yong, W. F.; Chung, T. Development of high performance carboxylated PIM-1/P84 blend membranes for pervaporation dehydration of isopropanol and CO_2/CH_4 separation. *J. Membr. Sci.* **2016**, *518*, 110-119.

(31) Panapitiya, N. P.; Wijenayake, S. N.; Nguyen, D.; Huang, Y.; Musselman, I. H.; Balkus, K. J.; Ferraris, J. P. Gas Separation Membranes Derived from High Performance Immiscible Polymer Blends Compatibilized with Small Molecules. *ACS Appl. Mater. Interfaces* **2015,** *7(33)***,** 18618–18627.

(32) Yong, W.; Li, F.; Xiao, Y.; Li, P.; Pramoda, K.; Tong, Y.; Chung, T. Molecular engineering of PIM-1/Matrimid blend membranes for gas separation. *J. Membr. Sci.* **2012**, *407-408*, 47-57.

(33) Mei Wu, X.; Gen Zhang, Q.; Ju Lin, P.; Qu, Y.; Mei Zhu, A.; Lin Liu, Q. Towards enhanced CO_2 selectivity of the PIM-1 membrane by blending with polyethylene glycol, *J. Membr. Sci.* **2015**, *493*, 147-155.

(34) Naderi, A.; Asadi Tashvigh, A.; Chung, T.; Weber, M.; Maletzko, C. Molecular design of double crosslinked sulfonated polyphenylsulfone /polybenzimidazole blend membranes for an efficient hydrogen purification, *J. Membr. Sci.* **2018**, *563*, 726-733.

(35) Yong, W. F.; Lee, Z. K.; Chung, T.; Weber, M.; Staudt, C.; Maletzko, C. Blends of a polymer of intrinsic microporosity and partially sulfonated polyphenylenesulfone for gas separation. *ChemSusChem* **2016**, *15*, 1953-1962.

(36) Park, K. S.; Ni, Z. N.; Coˆ te, A. P.; Choi, J. Y.; Huang, R.; Uribe-Romo, F. J.; Chae, H. K.; O'Keeffe, M.; Yaghi, O. M. Exceptional chemical and thermal stability of zeolitic imidazolate frameworks. *PNAS* **2006**, *27*, 10186-10191.

(37) Carta, M.; Malpass-Evans, R.; Croad, M.; Rogan, Y.; Jansen, J. C.; Bernardo, P.; Bazzarelli, F.; McKeown, N. B. An efficient polymer molecular sieve for membrane gas separations. *Science* **2013**, *6117*, 303-307.

(38) Carta, M.; Malpass-Evans, R.; Croad, M.; Rogan, Y.; Lee, M.; Rose, I.; McKeown, N. B. The synthesis of microporous polymers using Tröger's base formation. *Polym. Chem.* **2014**, *18*, 5267-5272.

(39) Tocci, E.; De Lorenzo, L.; Bernardo, P.; Clarizia, G.; Bazzarelli, F.; Mckeown, N. B.; Carta, M.; Malpass-Evans, R.; Friess, K.; Pilnáček, K. Molecular Modeling and Gas Permeation Properties of a Polymer of Intrinsic Microporosity Composed of Ethanoanthracene and Tröger's Base Units. *Macromolecules* **2014**, *22*, 7900-7916.

(40) Liédana, N.; Galve, A.; Rubio, C.; Téllez, C.; Coronas, J. CAF@ ZIF-8: one-step encapsulation of caffeine in MOF. *ACS Appl. Mater. Interfaces* **2012**, *9*, 5016-5021.

(41) Shao, L.; Chung, T.; Wensley, G.; Goh, S. H.; Pramoda, K. P. Casting solvent effects on morphologies, gas transport properties of a novel 6FDA/PMDA–TMMDA copolyimide membrane and its derived carbon membranes, *J. Membr. Sci.* **2004**, *1*, 77-87.

(42) Sánchez-Laínez, J.; Zornoza, B.; Téllez, C.; Coronas, J. Asymmetric polybenzimidazole membranes with thin selective skin layer containing ZIF-8 for H_2/CO_2 separation at pre-combustion capture conditions, *J. Membr. Sci.* **2018**, *563*, 427-434.

(43) Yong, W. F.; Chung, T. Miscible blends of carboxylated polymers of intrinsic microporosity (cPIM-1) and Matrimid. *Polymer* **2015**, *59*, 290-297.

(44) Fox T.G. ,*Bull Am Phys Soc* **1957**, 123.

(45) Svoboda, R.; Málek, J. Is the original Kissinger equation obsolete today? *J. Therm. Anal. Calorim.* **2014**, *2*, 1961-1967.

(46) Cacho-Bailo, F.; Téllez, C.; Coronas, J. Interactive thermal effects on metal–organic framework Polymer composite membranes. *Chem.-A Europ. J.* **2016**, *28*, 9533-9536.

(47) Drolet, D. P.; Manuta, D. M.; Lees, A. J.; Katnani, A.; Coyle, G. J. FT-IR and XPS study of copper (II) complexes of imidazole and benzimidazole. *Inorg. Chim. Acta* **1988**, *2*, 173-180.

(48) Wang, K. Y.; Chung, T.; Rajagopalan, R. Dehydration of tetrafluoropropanol (TFP) by pervaporation via novel PBI/BTDA-TDI/MDI co-polyimide (P84) dual-layer hollow fiber membranes. *J. Membr. Sci.* **2007**, *1*, 60-66.

(49) Sridhar, S.; Veerapur, R.; Patil, M.; Gudasi, K.; Aminabhavi, T. Matrimid polyimide membranes for the separation of carbon dioxide from methane. *J. Appl. Polym. Sci.* **2007**, *3*, 1585-1594.

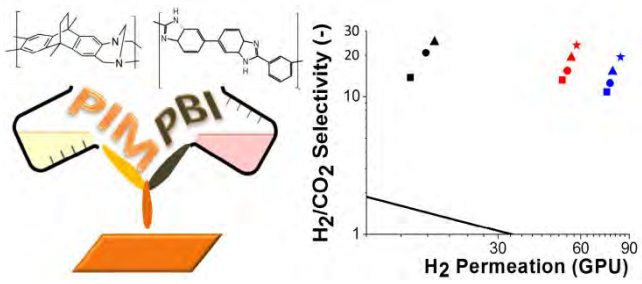
PIM
PBI
H_2/CO_2 Selectivity (-)
30
20
10
1
30
60
90
H_2 Permeation (GPU)

TOC graphic